Influences of dissolved oxygen sensor position on aeration efficiency of Venturi air injectors in aquaculture and wastewater treatment

Nantawat Demeekul[1], Kritsada Puangsuwan[2*], Eknarin Rodcharoen[3], Kuaanan Techato[1], Anil Kumar[4]

(1. *Faculty of Environmental Management, Prince of Songkla University, Songkhla 90112, Thailand*;
2. *Faculty of Science and Industrial Technology, Prince of Songkla University, Surat Thani Campus, Surat Thani, 84000, Thailand*;
3. *Faculty of Natural Resources, Prince of Songkla University, Songkhla 90112, Thailand*;
4. *Department of Mechanical Engineering, Delhi Technological University, Delhi, 110042, India*)

Abstract: This article concentrates on the aeration efficiency of venturi air injectors in aquaculture or wastewater treatment. This study was designed to investigate the location of the dissolved oxygen (DO) sensor installation, with a focus on investigating the aeration mechanism by studying ten variables, including temperature, pH, oxidation-reduction potential (ORP), electrical conductivity, resistivity, total dissolved solids, salinity, pressure, dissolved oxygen, and the effect of changing the position of DO sensor installations in different locations via oxygen transfer. The water temperature was raised due to the heating of the water pump. It ranged from 29.7°C to 32.78°C, with different temperatures resulting in different oxygen solubility. The pH level increased with the rise in oxygen levels due to an increase in OH^- concentration, whereas the ORP decreased when oxygen levels rose, increasing the reduction reaction. A study on the effect of changing the position of DO sensor installations in different locations was discovered using oxygen transfer coefficients (K_{La}) variables. The K_{La} values at nozzle depths of 15 cm, 30 cm, and 45 cm were 0.0004±0.0001, 0.000 42±0.0001, and 0.001 36±0.000 13, respectively. Therefore, there is a slight difference of K_{La} value when changing the position of sensor installations. An inappropriate distance between the DO sensor and nozzle installation is able to cause turbulent flow. This event resulted in an incorrect DO value. Moreover, the installation of the DO sensor too far from the nozzle resulted in a low value of DO.

Keywords: venturi aspirator, aeration systems, aeration efficiency, dissolved oxygen, position of DO sensor, DO sensor
DOI: 10.25165/j.ijabe.20251803.8962

Citation: Demeekul N, Puangsuwan K, Rodcharoen E, Techato K, Kumar A. Influences of dissolved oxygen sensor position on aeration efficiency of Venturi air injectors in aquaculture and wastewater treatment. Int J Agric & Biol Eng, 2025; 18(3): 58–62.

1 Introduction

Due to increasing food demand, countries are prioritizing the expansion and enhancement of their aquaculture and agriculture sectors to meet global food needs[1]. The aquaculture industry plays a crucial role in addressing these demands, with a focus on maintaining water quality parameters, particularly dissolved oxygen (DO), for healthy aquatic life in ponds[2,3]. Various mechanical techniques, such as waterwheel aerators, jet aerators, and bubble diffusers, are employed to aerate water efficiently. Selecting the right aerator is essential for economic efficiency and meeting oxygen requirements[4]. Propeller-aspirator-pump aerators, utilizing the venturi concept, have gained attention for their ability to enhance oxygen content in water bodies, particularly in recirculating aquaculture systems, benefiting hydraulic and environmental engineering[5,6].

This study is exploring the development of a Smart Aquaculture system. Understanding the dynamics of water quality, particularly in relation to dissolved oxygen (DO) levels and the optimal placement of DO sensors, is crucial for effective aeration. This research aims to investigate the placement of DO sensors by assessing various variables including temperature, pH, oxidation-reduction potential (ORP), electrical conductivity (EC), resistivity, total dissolved solids (TDS), salinity, pressure, and dissolved oxygen. Additionally, This study will examine how changing the positioning of DO sensors affects oxygen transfer coefficients. This guideline ensures precise DO measurement and the application of venturi aerators and IoT systems in Recirculating Aquaculture Systems (RAS) for efficient aquaculture practices.

2 Theory and formula

2.1 Oxygen transfer

The conversion of oxygen from gas to liquid form is referred to as oxygen transfer. This process is quantified by the volumetric mass transfer coefficient (K_{La}), as described in Equation (1). K_{La} correlates with the rate at which oxygen concentration increases in the liquid, reaching equilibrium under specific temperature and atmospheric pressure conditions.

$$\frac{\mathrm{d}C}{\mathrm{d}t} = K_{La} \cdot (C_S - C_0) \tag{1}$$

where, $\frac{\mathrm{d}C}{\mathrm{d}t}$ is oxygen transfer differential; C_S is the saturated

Received date: 2024-03-27 **Accepted date:** 2025-03-16
Biographies: **Nantawat Demeekul**, PhD candidate, research interest: waste water treatment system, Email: nd-mne@hotmail.com; **Eknarin Rodcharoen**, Assistant Professor, research interest: marine and coastal ecology, Email: eknarin.r@psu.ac.th; **Kuaanan Techato**, Associate Professor, research interest: energy and environment management, Email: kuaanan.t@psu.ac.th; **Anil Kumar**, Professor, research interest: clean energy and energy transition, Email: anilkumar76@dtu.ac.in.

***Corresponding author: Kritsada Puangsuwan**, Assistant Professor, research interest: electronics technology for agriculture. Faculty of Science and Industrial Technology, Prince of Songkla University, Surat Thani Campus, Surat Thani, 84000, Thailand, Tel: +660-840524595, Email: kritsada.pu@psu.ac.th.

dissolved O_2 mass concentration in the liquid at the steady-state point, mg/L; C_0 is the O_2 concentration in the liquid phase at the start of the experiment, mg/L; and K_{La} is the system's mass transfer coefficient, h^{-1}.

Equation (2) is obtained by integrating Equation (1), allowing the total mass transfer coefficient K_{La} to be calculated in relation to the total volume of liquid in the system.

$$\ln(C_S - C_i) = K_{La} \cdot T \quad (2)$$

where, C_i is the O_2 concentration in the liquid phase at time t, mg/L; K_{La} is the mass transfer coefficient of the system at water temperature T, h^{-1}; and t is the time, h. The coefficient K_{La} is the slope of the regression line derived from the relationship between the logarithmic function and time.

2.2 Aeration equipment test

The aerator was employed in different situations. Due to the obvious differences in operating conditions, the findings cannot be directly compared. As a result, the air equipment test was carried out by putting the aerator through its paces under controlled conditions.

The analysis method comprised measuring the oxygen transfer rate in the dissolved oxygen mass unit per unit of time in the volume of water tested, according to the American Society of Civil Engineers' standardized measurement of oxygen transfer in clean water[7].

Sodium sulfites were utilized in the test as a reaction to dissolved oxygen, resulting in zero oxygen in the water. Equations (3)-(5) show how to use cobalt chloride as a catalyst.

$$Na_2SO_3 + 0.5O_2 \rightarrow 2Na_2SO_4 \quad (3)$$

$$\text{The amount of sodium sulfite required} = \frac{8\text{mg}Na_2SO_3}{1\text{mg}O_2} \times 1.15 \quad (4)$$

$$\text{The amount of cobalt chloride required} = \frac{0.5\text{mg}COCl_2}{1\text{ Literof Water}} \frac{0.5\text{mg}COCl_2}{1\text{ Literof Water}} \quad (5)$$

The aerator continuously monitors the increase in dissolved oxygen levels throughout the test, recording the rate of oxygen dissolved per unit of time. The test halts once the water approaches saturation with oxygen. Multiple tests may be conducted using the same water. However, if the addition of deoxygenation chemicals causes the total dissolved solids (TDS) concentration to exceed 2000 mg/L, the test water (clean water) must be replaced. TDS and conductivity of the test water are measured using a conductivity meter upon completion of each test[7,8].

From Equation (1), where the researcher moves to the integral between the concentration periods at the start time, to the duration t, as in Equations (6) and (7), the recorded dissolved oxygen bill is evaluated for oxygen transfer coefficients (K_{La}).

$$\int_{C_0}^{C_t} \frac{1}{(C_s - C)} dc = K_{La} \cdot \int_0^t dt \quad (6)$$

$$\ln \frac{(C_s - C_0)}{(C_s - C_t)} = K_{La} \cdot t \quad (7)$$

When the oxygen concentration rises from zero, the test data can begin at approximately $C = 0.1\ C_{s,t}$. The test's endpoint should not be higher than $0.8\ C_{s,t}$. For the data analysis, at least 30 values should be collected. The desorption process necessitates a 10 mg/L higher start point than the saturation threshold. A graph of the relationship between $\ln \frac{(C_s - C_0)}{(C_s - C_t)}$ and time (t) is created, using Equation (7) to generate a linear relationship, with the slope of the plot indicating the value of oxygen transfer coefficients (K_{La}) [7].

The DO deficit was calculated by subtracting the measured DO concentration from saturation DO for each time interval. A regression equation was derived by plotting the natural logarithm of oxygen deficit against aeration time, with the slope representing the overall oxygen transfer coefficient (K_{La}). Using this equation, the time for DO concentration to reach 10% and 80% of saturation was calculated[9].

2.3 Experimental setup

The experiments were conducted using a recirculation system. Various equipment was used in the project, including the HANNA instruments® model HI 9829 multiparameter meter, PVC water supply pipes, venturi aspirators, a centrifugal pump (Model MCP158BR), water pressure gauges, glass rotor flowmeters, air mass flow controllers (PFM711-02-A), and tube aeration devices (Figure 1). Chemicals included Sodium sulfite anhydrous and Cobalt (II) chloride-6-hydrate. Water from a recirculation tank was injected into the venturi aspirator to circulate the tank perimeter. Test water (clean water) had controlled TDS concentrations below 2000 mg/L, and dissolved oxygen (DO) analysis was conducted before conditioning the water with chemicals[7].

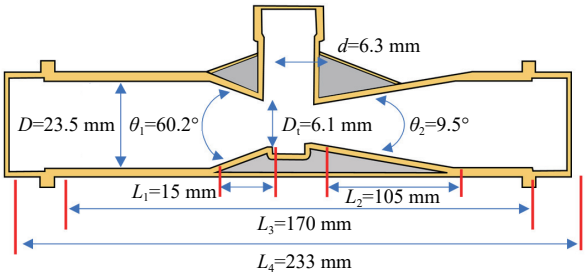

Figure 1 Schematic of venturi

In experiment, when pumping through a 1-inch venturi, it has a flow rate of 26 L/min, an air intake of 22.5 L/min, and a water pressure of 0.75 bar before entering the venturi.

2.4 Testing system

Experiments were conducted using 1.0-inch venturi sizes and a 0.746 kW pump in a recirculation tank holding approximately 560 L of water. Water was pumped through the venturi at a rate of 50 L/min. The water inlet depth varied at 15 cm, 30 cm, and 45 cm below the surface, with the DO sensor positioned at 90°, 180°, and 270°, as depicted in Figure 2. Data on the dependent variable were

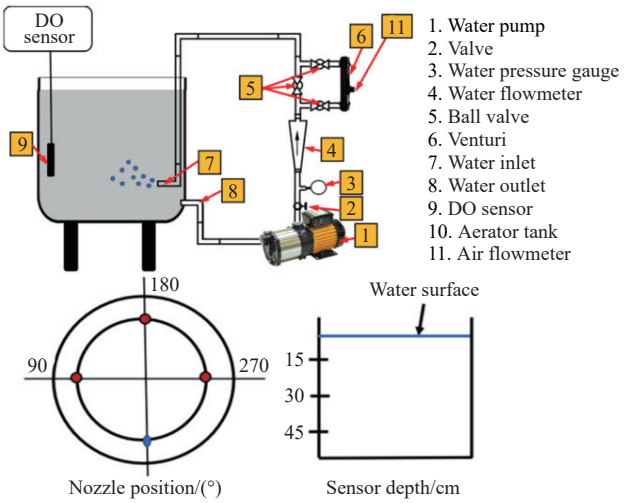

Figure 2 Installation of equipment in experiment

recorded and aeration efficiency tests were conducted following the American Society of Civil Engineers' standardized measurement of oxygen transfer in clean water to analyze the coefficient of oxygen transfer (K_{La})[7]. Each oxygen-transfer test was replicated three times. DO concentrations were measured at intervals of every 1 s, with each trial lasting a total duration of 5500 s to ensure all values exceeded 80% saturation, starting from near 0 mg/L.

3 Results and discussion

According to the study, the aeration mechanism results in changes in the variables. Table 1 shows the results when oxygenating the water.

Table 1 Summary of variables

Variables	Max	Min	Average	Standard deviation	Experimental status
Temp/°C	32.78	29.7	31.58	0.720	Increases as the duration increases due to the heat generated by the water pump.
pH	7.81	6.9	7.245	0.253	Increases when oxygen levels in the water rise, caused by increment of OH^- concentration, which causes the pH of water to increase.
ORP/mV	209.40	112.9	177.97	17.654	Decreases with increasing oxygen levels in the water, which results in an increase in the reduction reaction.
EC/μS\cdot cm^{-1}	266	202	254.89	11.41	There is no change when increasing the oxygen level in the water.
RES/Ohm-cm	4950	3759	3931.402	198.783	There is no change when increasing the oxygen level in the water.
TDS/ppm	133	101	127.44	5.734	There is no change when increasing the oxygen level in the water.
Sal./psu	0.12	0.09	0.12	0.005	There is no change when increasing the oxygen level in the water.
Press/psi	14.64	14.52	14.58	0.197	The experiment tends to increase the pressure, due to the increase in H_2O and OH− molecules in the water.
DO/ppm	7.16	0.13	5.03	1.606	The solubility of oxygen changes depending on the temperature.

Water temperature, ranging from 29.7°C to 32.78°C due to the pump's heat, affects oxygen solubility. At 33°C, solubility is 7.18 mg/L, consistent with research[10]. Increasing temperature slightly raises water conductivity (EC). Actually, dissolved oxygen (DO) decreases as temperature increases due to physical solubility principles. Primarily, the rise in temperature increases the kinetic energy of oxygen molecules, causing them to escape from the water, which reduces solubility. This phenomenon is governed by Henry's Law. Relationships between DO, pH, ORP, and pressure (Figures 3-5) highlight a correlation, especially between pH and DO. Factors like algal activity, temperature, and organic matter impact both parameters[11,12]. Under anaerobic conditions, all variables follow similar patterns. Clean water's oxidation-reduction properties, influenced by acidity, relate to a reversed electric motor principle. Disruption of magnetic flux generates electrons, inducing current[13]. In equilibrium, water dissociates into H^+ and OH^- ions as in Equation (8)[14].

$$H_2O \leftrightharpoons H^+ + OH^- \quad (8)$$

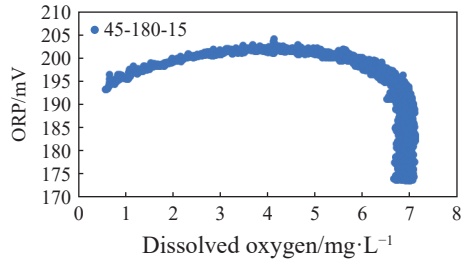

Figure 3 Changes in ORP with increasing oxygen in the water

After generating an electron, it forms a weak bond with the H^+ cation due to its negative charge [Equation (9)], increasing the OH^- concentration and raising the water's pH. This disrupts the equilibrium of Equation (10). According to Le Chatelier's principle, excess OH^- ions further dissociate into H_2O, O_2, and electrons (Equation (10)), leading to oxygen production in the water stream. This increase in dissolved oxygen levels was observed post-magnetic effect[15,16].

$$2H^+ + 2e^- \leftrightharpoons H_2(g) \quad (9)$$

$$O_2(g) + 4H^+ + 4e^- \leftrightharpoons 2H_2O(aq) \quad (10)$$

As pH decreases (i.e., the concentration or activity of H^+ increases), the redox reaction is shifted to the right. Hydrogen ions and oxygen react with water, which results in a decrease in the DO. An increase in the pH value can shift the redox reaction to the left[17,18].

In the reduction reactions involving oxyanions with a central redox-active atom, oxide anions (O^{2-}) being in excess are freed up when the central atom is reduced. The acid-base neutralization of each oxide ion consumes two H^+ or one H_2O molecule, as follows in Equations (11) and (12):

$$O^{2-} + 2H^+ \leftrightharpoons H_2O \quad (11)$$

$$O^{2-} + H_2O \leftrightharpoons 2OH^- \quad (12)$$

Therefore, when the reduction reaction of water increases, it will increase the exposure of electrons, which also results in a decrease in the ORP value in the water, as shown in Figure 3. However, based on the experiments, certain conditions do result in DO increases when pH has increased[19,20]. Furthermore, published correlations between pH and DO, No. 45-180-15 (nozzle depth 45 cm, nozzle position 180°, and sensor depth 15 cm) are shown in Figure 4. Thereby, when oxygen is added to the water, it causes the increase in the pH of the water as well.

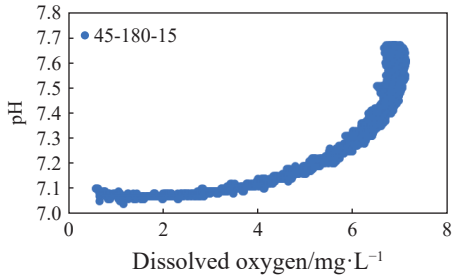

Figure 4 Changes in pH with increasing oxygen in the water

The pressure of the water slightly increased when adding oxygen, as shown in Figure 5. However, the pressure tends to increase because chemical reactions proceed at vastly different speeds depending on the oxygen content transformation, the temperature, and other factors. When high oxygen is added, the

molecular content of H_2O and OH^- is dissolved up to the point of saturation, which increases the density of water, causing the pressure acting on the sensor to increase.

Experiments indicate minimal changes in EC, RES, TDS, and Sal. While water temperature has a slight impact, it is notable that both conductivity (EC) and resistivity (RES) are measures of a fluid's electrical conductivity. Conductivity is significantly affected by temperature fluctuations[21].

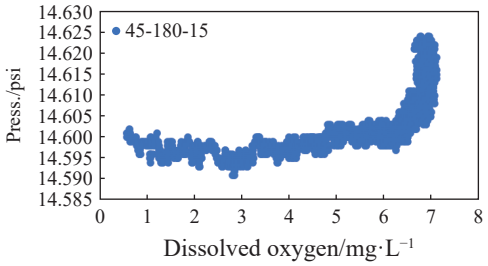

Figure 5 Changes in pressure with increasing oxygen in the water

Temperature typically affects the resistance and electrical resistivity of materials. Changes in electrical resistance can significantly impact various electrical and electronic circuits. The temperature coefficient of resistance is crucial in understanding these effects. It is defined as the change in electrical resistance per degree change in temperature. Conductor resistance depends on electron collision processes within the material. As temperature rises, electron collisions become more frequent and faster, leading to increased resistance in the conductor[22].

Let us consider that the resistance of a conductor at 0°C is R_0 and at temperature T (°C) is R_T. The relation between temperature and resistances R_0 and R_T is approximately given as Equations (13) and (14).

$$R_T=R_0[1+\alpha(T-T_0)]; \tag{13}$$

$$R_T=R_0[1+\alpha(\Delta T)] \tag{14}$$

Temperature's impact on electrical resistance relies on three key factors: the initial resistance value, temperature increase, and the temperature coefficient of resistance (α). This phenomenon extends to the conductivity of solutions, which is influenced by temperature-induced changes in viscosity and ion behavior. Generally, conductivity rises with increasing temperature[23].

Conductivity or electrical conductivity (EC) and total dissolved solids (TDS) are frequently used as water quality parameters[24]. Electrical conductivity is widely applied as a basic tool to assess water quality. The relationship between total dissolved solids (TDS) (mg/L) and EC (μS/cm) is often described by a parameter that varies according to chemical composition: TDS = A × EC, where the constant A is in the range of 0.55 to 0.9 in most conductivity meters, reflecting the unique molar masses and charges of the most common anions: Cl^-, HCO_3^- and SO_4^{2-}. Typically, this parameter is high for Cl^- rich waters and low for SO_4^{2-} rich waters[17,25]. Researchers have studied the correlation between EC and TDS in various types of water. We found that fresh water, EC = 300-800 μS/cm has a ratio TDS/EC (in 25°C) at 0.55. This is in line with our research, where the average ratio of EC and TDS is 0.5 at 29.7°C-32.78°C, which is similar and does not change when oxygen content is added[26].

This study has demonstrated the influence of changing the position of DO sensor installations in different locations. The nozzle depths were designed at 15, 30, and 45 cm. Each nozzle depth was separated into three angles, including 90°, 180°, and 270° in 15 cm, 30 cm, and 45 cm of sensor depth. At nozzle depths of 15 cm and 30 cm, the K_{La} value ranges between 0.0003 and 0.0005, averaging 0.0004, whereas at a depth of 45 cm, it ranges from 0.0011 to 0.0015, averaging 0.0014. Notably, the K_{La} value at the 45 cm depth is higher compared to other depths, while the highest value occurs at a distance of 30 cm (Table 2). This discrepancy in K_{La} values suggests that the sensor's installation distance relative to the nozzle is a crucial factor. Specifically, positioning the sensor at a distance of 30 cm yields the highest K_{La} value. Furthermore, when installing the sensor perpendicular to the nozzle, the distance should also be taken into account.

Table 2 K_{La} value in different depths

Nozzle depths/cm	K_{La} value		
	Range	Average	Standard deviation
15	0.0003 - 0.0005	0.0004	7.07E-05
30	0.0003 - 0.0005	0.0004	6.67E-05
45	0.0011 - 0.0015	0.0014	13.33E-05

However, when considering the installation distance of the sensor at angles of 180° and 270° relative to the nozzle, it was observed that the K_{La} value was highest at a sensor depth of 15 cm. Additionally, measurements taken at a sensor distance of 270° revealed varying K_{La} values across different depths[9,27,28].

This study highlights the impact of sensor installation position on K_{La} values, demonstrating slight differences when positions were altered. For instance, the average K_{La} at a nozzle depth of 45 cm was 0.0136, compared to 0.004 and 0.0042 at depths of 15 cm and 30 cm, respectively. This suggests that increasing the space and time for air bubbles to reach the water surface enhances oxygen transfer in water[29].

During the initial turbulent flow phase from the nozzle, mass transfer primarily occurred through convective processes. This involved the exchange of oxygen between moving air and water, likely due to water impact. In contrast, molecular diffusion flow, characterized by laminar flow, facilitated mass transfer through random motion within a stationary medium along the water flow. In the experiment, water mixed with air flowed to the tank bottom through an outlet[30]. At a sensor depth of 30 cm, the highest K_{La} value was observed, indicating optimal water-air mixing. This suggests that sensor placement at this depth maximizes water-air interaction. Sensor placement at depths up to 30 cm at nozzle depths of 15 cm and 30 cm, and at 45 cm at 90° from the nozzle, proved effective. However, at a nozzle depth of 45 cm, particularly at 180° and 270°, the best K_{La} was achieved at a sensor depth of 15 cm due to higher air volume, affecting sensor-nozzle distance.

4 Conclusions

The study found that motor-generated heat raises temperature, reducing dissolved oxygen solubility in freshwater. Oxygen addition increases pH, affecting ORP and inducing chemical reactions. Rising water density due to increased oxygen solubility elevates pressure on the sensor. Temperature also affects solution conductivity, altering viscosity and ion behavior. DO sensor placement variations showed slight K_{La} differences. Notably, nozzle depth significantly impacts aeration, suggesting avoidance of sensor placement near the nozzle due to turbulent flow.

Acknowledgements

This research was made possible through generous support

from the Faculty of Environmental Management, as well as the High-Potential Talent Fund to strengthen capabilities in the economic, social, and community sectors (Talent Utilization) Type 2 No.TU1-10/2564 from the Graduate School, Prince of Songkla University (PSU). The authors extend their sincere gratitude to the Southern Industrial Pollutions Research and Warning Center (DIW, Department of Industrial Works) for their invaluable academic guidance, technical resources, and facility support throughout this study.

[References]

[1] Henriksson P J G, Troell M, Banks L K, Belton B, Beveridge M C M, Klinger D H, et al. Interventions for improving the productivity and environmental performance of global aquaculture for future food security. One Earth, 2021; 4(9): 1220–1232.

[2] Boyd C E, D'Abramo L R, Glencross B D, Huyben D C, Juarez L M, Lockwood G S, et al. Achieving sustainable aquaculture: Historical and current perspectives and future needs and challenges. Journal of the World Aquaculture Society, 2020; 51(3): 578–633.

[3] Zhang X, Zhang Y, Zhang Q, Liu P, Guo R, Jin S, et al. Evaluation and analysis of water quality of marine aquaculture area. International Journal of Environmental Research and Public Health. 2020; 17(4): 1446. DOI: 10.3390/ijerph17041446

[4] Xiao R, Wei Y, An D, Li D, Ta X, Wu Y, et al. A review on the research status and development trend of equipment in water treatment processes of recirculating aquaculture systems. Reviews in Aquaculture, 2019; 11(3): 863–895.

[5] Mahmud R, Erguvan M, MacPhee D W. Performance of closed loop venturi aspirated aeration system: experimental study and numerical analysis with discrete bubble model. Water, 2020; 12(6): 1637.

[6] Zhang C, Song B, Shan J, Ni Q, Wu F, Wang S. Design and optimization of a new tube aeration device. Aquaculture international. 2020; 28: 985–99. DOI: 10.1007/s10499-020-00507-2

[7] Engineers ASoC, editor. Measurement of oxygen transfer in clean water. American Society of Civil Engineers, 1993. DOI: 10.1061/978087262885

[8] Eckenfelder W W, Boero V J, Flippin T H, editors. The effect of high TDS on the activated sludge process. Water Environment Federation, Weftec Latin America, 2001: DOI: 10.2175/193864701784293170

[9] Laksitanonta S, Singh G. Design of a combined propeller and venturi tube system for aquaculture ponds. Agriculture and Natural Resources, 2004; 38(2): 267–277.

[10] Benson B B, Krause Jr D. The concentration and isotopic fractionation of oxygen dissolved in freshwater and seawater in equilibrium with the atmosphere 1. Limnology and oceanography, 1984; 29(3): 620–632.

[11] Scholz M. Wetland systems to control urban runoff. Elsevier, 2015.

[12] León Robles A, Acedo Félix E, Gomez-Gil B, Quiñones Ramírez EI, Nevárez-Martínez M, Noriega-Orozco L. Relationship of aquatic environmental factors with the abundance of Vibrio cholerae, Vibrio parahaemolyticus, Vibrio mimicus and Vibrio vulnificus in the coastal area of Guaymas, Sonora, Mexico. Journal of Water and Health, 2013; 11(4): 700–712.

[13] Wang Q A, Huang S D, Sun T Y. Study on the coordinate periodic change and the relativity between pH and DO in shallow water with algae. Sichuan Environment, 2001; 20(2): 4–7, 29. (in Chinese)

[14] Lee S, Rasaiah J C. Proton transfer and the mobilities of the H^+ and OH^- ions from studies of a dissociating model for water. The Journal of Chemical Physics, 2011; 135(12). DOI: 10.1063/1.3632990

[15] Zang C J, Huang S L, Wu M, Du S L, Scholz M, Gao F, et al. Comparison of relationships between pH, dissolved oxygen and chlorophyll a for aquaculture and non-aquaculture waters. Water, Air, & Soil Pollution, 2011; 219: 157–174.

[16] Matsushima H, Iida T, Fukunaka Y, Bund A. PEMFC performance in a magnetic field. Fuel Cells, 2008; 8(1): 33–36.

[17] Liu J, Wang L, Lin X, Zhang R. Influence of different O_2/H_2O ratios on He atmospheric pressure plasma jet impinging on a dielectric surface. Journal of Physics D: Applied Physics, 2021; 55(12): 125203.

[18] Pang S C, Chin S F, Anderson M A. Redox equilibria of iron oxides in aqueous-based magnetite dispersions: Effect of pH and redox potential. Journal of Colloid and Interface Science, 2007; 311(1): 94–101.

[19] Lee H S, Yap A C W, Ng C C, Mohd N S, Loo J L, editors. Increased electron density and dissolved oxygen level in water through magnetic effect. IOP Conference Series: Earth and Environmental Science; 2019: IOP Publishing. DOI: 10.1088/1755-1315/257/1/012010

[20] Tomasetti S J, Gobler C J. Dissolved oxygen and pH criteria leave fisheries at risk. Science, 2020; 368(6489): 372–373.

[21] Rodríguez-Rodríguez M, Fernández-Ayuso A, Hayashi M, Moral-Martos F. Using water temperature, electrical conductivity, and pH to Characterize surface–groundwater relations in a shallow ponds system (Doñana National Park, SW Spain). Water, 2018; 10(10): 1406.

[22] Wen Y, Chen C, Ye Y, Xue Z, Liu H, Zhou X, et al. Advances on thermally conductive epoxy‐based composites as electronic packaging underfill materials—A review. Advanced Materials, 2022; 34(52): 2201023.

[23] Burger N, Laachachi A, Ferriol M, Lutz M, Toniazzo V, Ruch D. Review of thermal conductivity in composites: Mechanisms, parameters and theory. Progress in Polymer Science, 2016; 61: 1–28.

[24] Dewangan S, Kadri M, Saruta S, Yadav S, Minj N. Temperatireture effect on electrical conductivity (EC) & total dissolved solids (TDS) of water: A review. International Journal of Research and Analytical Reviews (IJRAR), 2023; 10(2): 514–520.

[25] Parker E V, COUTURIER M, BENFEI T. Oxygen management at a commercial freshwater recirculating aquaculture system: University of New Brunswick, 2000.

[26] Marandi A, Polikarpus M, Jõeleht A. A new approach for describing the relationship between electrical conductivity and major anion concentration in natural waters. Applied geochemistry, 2013; 38: 103–109.

[27] Thakre S, Bhuyar L, Deshmukh S. Effect of different configurations of mechanical aerators on oxygen transfer and aeration efficiency with respect to power consumption. International Journal of Aerospace and Mechanical Engineering. 2008; 2(2): 100–108.

[28] Ozkan F, Ozturk M, Baylar A. Experimental investigations of air and liquid injection by venturi tubes. Water and Environment Journal, 2006; 20(3): 114–122.

[29] Asgharpour M, Mehrnia M R, Mostoufi N. Effect of surface contaminants on oxygen transfer in bubble column reactors. Biochemical Engineering Journal, 2010; 49(3): 351–360.

[30] Jahromi M E, Khiadani M. Experimental study on oxygen transfer capacity of water jets discharging into turbulent cross-flow. Journal of Environmental Engineering, 2017; 143(6): 04017007.